Low insertion loss and switching energy all-optical gate for 40 Gbit/s WDM networks

D. Massoubre[a], J. Dion[a], J. Landreau[b], J. Decobert[b], A. Shen[b] and J.-L. Oudar[a]

[a]LPN-CNRS, Route de Nozay, 91460 Marcoussis, France.
[b]Alcatel-Thales III-V Lab, Route de Nozay, 91460 Marcoussis, France.

ABSTRACT

A very low-loss and low switching energy vertical micro-cavity has been developed for all-optical signal reshaping. This saturable absorber-based device shows insertion loss as low as 0.2 dB and a switching energy of 13 $\mu J/cm^2$ while keeping a response time lower than 5 ps. Such a low loss and low switching energy device has high potential applications in 2 R regenerated transmission lines.

Keywords: Fabry-Perot micro-cavity, saturable absorber, regeneration, all-optical device, non-linear optics, optical signal processing

1. INTRODUCTION

All-optical communication systems with ultra-high capacities and long-haul transmission distances need a number of signal processing steps to overcome the propagation impairments. These steps are the Re-amplifying, the Re-shaping and Re-timing, also referred to as 3R-regeneration (2 R-regeneration if the Re-timing step is skipped).[1] Because of the increasing complexity of opto-electronic devices with bit rate and of their speed limitations, all-optical devices are very attractive for low-cost in-line signal processing.[2,3] All-optical components achieving the re-shaping step are a key element in the regeneration reliability as they perform the optical decision between logical ones and zeros. These devices need a non-linear intensity transfer function (output power versus input power) to perform their non-linear gate role. The ideal transfer function is the step function, which is physically impossible. Different nonlinear optical gates approaching more or less the ideal response have been realized in various media such as fiber-based Non-linear Optical Loop Mirror[4](NOLM), semiconductor optical amplifier (SOA)-based interferometers,[5] electro-absorption modulator,[6] passive saturable absorbers (SAs)[7] and bistable laser.[8] These non-linear gates work either by cross-regeneration, i.e. the data are transferred from one wavelength to another one (wavelength conversion), either by self-regeneration, i.e. the data are self-modulated. Among these non-linear gates, the SA-based gates have raised considerable interest for all-optical switching in particular, due to their large non-linear optical effect, their integration facilities and their fully passive operating mode (no bias-voltage, nor Peltier cooler), so potentially low cost. For these SA-based gates the non-linear transfer function is achieved by modulation of carrier density in the active region. InP-based multiple-quantum-well saturable absorbers (MQW-SA) are currently investigated for optical telecommunication signals processing because one easily gets an absorption peak at 1.55 μm,[7,9–11] but recently GaAs-based MQW-SA[12] and carbon-nanotube-based SA[13] have also been investigated.

To be used like a low-cost regenerator at high bit-rate, MQW-SA-based gates must combine numerous characteristics such a switching energy and insertion loss as low as possible, a contrast ratio around 4 dB, an ultra-fast recovery time (typically 5 ps for 40 Gbit/s transmission lines). They need to be polarisation-insensitive, easy to make and compatible with wavelength division multiplexed (WDM) systems. To amplify the non-linear response and to reduce the switching energy, MQW-SAs are included inside an asymmetric Fabry-Perot microcavity. The use of microcavity effects combined with excitonic absorption enhances the effective nonlinearity, and thus contributes to the reduction of the switching energy.[14] Furthermore, it is to be used at normal incidence, thus yielding intrinsic polarisation-insensitive operation. MQW-SAs present intrinsically a

Further author information: (Send correspondence to D. Massoubre)
E-mail: David.Massoubre@lpn.cnrs.fr, Phone: (0033) 169 636 154
Website: www.lpn.cnrs.fr

Photonics, Devices, and Systems III,
edited by Pavel Tománek, Miroslav Hrabovský, Miroslav Miler, Dagmar Senderáková,
Proc. of SPIE Vol. 6180, 61801N, (2006) · 0277-786X/06/$15 · doi: 10.1117/12.675742

long recovery time in the nanosecond range. To strongly decrease the response time of these materials we can introduce capture and recombination centers during or after the crystal growth via low-temperature molecular beam epitaxy,[15] high-energy ion implantation[16] or Be- or Fe-doping.[17,18] These methods of damage creation have been reported to provide recovery times as short as a few picoseconds (ps) on InP-based semiconductor.[16]

The combination of heavy-ion irradiation with a compact microcavity comprising a metallic (silver) back mirror has proved to be a convenient solution for making efficient optical gates.[10] Compared to all-semiconductor high reflectance Bragg mirror, this silver-based broadband mirror, deposited after the irradiation step, presents two decisive advantages. Firstly it gives a much higher bandwidth, essential for WDM processing, and secondly it is irradiation insensitive. Indeed, as the irradiation step is a post-growth process, the all-semiconductor Bragg mirror would undergo an ion implantation leading to a strong residual absorption[19] and thus a higher insertion loss. Such a device has shown an important improvement of the propagation distance in 40 Gbit/s long-haul transmission lines[20] but with an extinction ratio of only 2.5 dB, insertion loss of 8 dB (circulator included) and input power of 15 dBm. Higher extinction ratio have been reported but at lower bit rate and to the detriment of insertion loss.[21]

To reduce the switching energy, it is necessary to increase the cavity finesse. This may be reached by reducing the active layer thickness and/or by increasing the back mirror reflectance.[14] Recently, we developed devices with only 3 MQW-saturable absorber[22] while keeping a silver back mirror in order to keep a bandwidth large enough and leading to a cavity finesse of 16. Unfortunately we showed that insertion loss (i.e. the device non-saturable loss) were increased, because of the back mirror loss enhancement at increased finesse. To minimize these insertion loss while keeping a low switching energy, we must increase the back mirror reflectance while reducing the active layer thickness.

We report here on a new saturable absorber device made with a low-loss broadband metal-based back mirror to enhance these overall performances. The basic device structure is similar to the one reported elsewhere.[22,23] It consists of a thin irradiated MQW-SA active layer comprised inside an asymmetric Fabry-Perot microcavity. The originality of this new work is to use a low-loss broadband high reflectance back mirror to increase the microcavity finesse yielding to lower insertion loss. The characteristics measured on this device gave insertion loss lower than 0.3 dB, a maximum contrast ratio of 8.5 dB, a switching energy of 13 μJ/cm^2 and a bandwidth higher than 30 nm.

2. DESIGN AND FABRICATION

From the epitaxy to the final device, the process necessitates 7 steps we describe below. The as-grown structure and the final device are schematized on the figures 1.a and 1.b respectively. The semiconductor structure used in this study was grown by metalorganic vapour phase epitaxy (MOVPE) on InP substrate. The layer thicknesses were calculated to work at 1.55 μm with either a silver back mirror or a broadband silver-based back mirror. The growth incorporated a 500 nm-thick InP buffer layer, followed by an InGaAsP etch-stop layer (Eg $\approx$ 0.87 eV). Then an InP phase layer (PL1) has been deposited, followed by the active layer consisting of 7$\times$InGaAs (Eg $\approx$ 0.8 eV) 10 nm-thick quantum wells, sandwiched between 8$\times$InAlAs (Eg $\approx$ 1.45 eV) 7 nm-thick barriers, resulting in a MQW excitonic absorption peak at $\sim$ 1550nm The structure was completed by a phase bi-layers (PL2) comprising a thin InP layer followed by an InGaAsP layer (Eg $\approx$ 0.87 eV). As the back mirror deposition is a post-growth step, the as-grown structure is upside down. The PL2 bi-layer is used to place the saturable absorber section at the antinode of the intracavity intensity while the PL1 layer allows us to get the resonance matching, i.e. no phase displacement at the working wavelength. This design, with a resonant absorber section, ensures a stronger and more uniform coupling of the saturable absorber quantum well structure with the optical signal, therefore enhancing the effective nonlinearity.

As mentioned above, the sample is then irradiated to shorten the recovery time to a few picoseconds. The irradiation has been done with Ni^{6+} ions at 12 MeV, with irradiation dose of $1 \times 10^{11}\, cm^{-1}$, using the ARAMIS High Energy Ion Implanter at the University of Orsay, France. During irradiation, the sample was tilted by 7 degrees from normal incidence to minimise channeling effects. Such energetic heavy-ions are implanted deeply into the InP substrate (estimated depth of 4-5 μm), clusters of point defects are thus created along the implanting ion path through the active layer leading to efficient recombination centers, which reduce the carrier lifetime

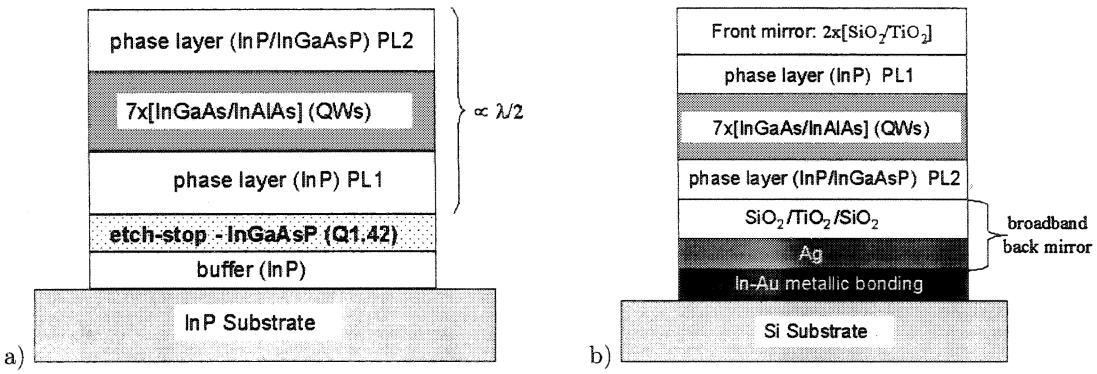

Figure 1. As-grown (a) and final device (b) structure.

from a few nanoseconds to a few picoseconds.[24] After irradiation, the Ag-based broadband mirror was deposited on the epitaxial structure. This back mirror consists of $SiO_2/TiO_2/SiO_2$ $[0.25 \times \lambda : 0.25 \times \lambda : 0.226 \times \lambda]$ layers deposited by electron beam evaporation (EBE), followed by an ultrathin (<4 nm) Chromium (Cr) bonding layer and a 300 nm-thick Ag layer, both of them deposited by vacuum thermal evaporation (VTE). Such a mirror has theoretically a reflectance higher than 99 %. In order to fabricate the vertical microcavity, a top-down mounting of the structure is now necessary. This was done by transferring the sample with a bonding layer on a new substrate of Si. This bonding is an important step because the bonding layer must provides mechanical support, a good heat dissipation, a low-process temperature to reduce stress on the bonded structure and recombination centers annihilation. A die bonding with an Indium-Gold (In-Au) isothermal solid-liquid interdiffusion (SLID) technique was used to achieved this bonding layer.[25] It consists to form an Au-In eutectic alloy. We deposited by evaporation Ti/Au/In/Au [30/600/150/20] nm-thick layers on the Si substrate and Ti/Au [30/150] nm-thick layers on the sample. Then the Si-substrate is joined to the Au-coated sample with enough pressure to allow intimate contact, at a temperature above 157 °C. Above this temperature, the indium layer melts and dissolves the gold layers to form a mixture of liquid and solid. The solid-liquid interdiffusion process continues until the mixture solidifies to form the Au-In eutectic bond. The resulting bond has an unbonding temperature greater than 500 °C.[25]

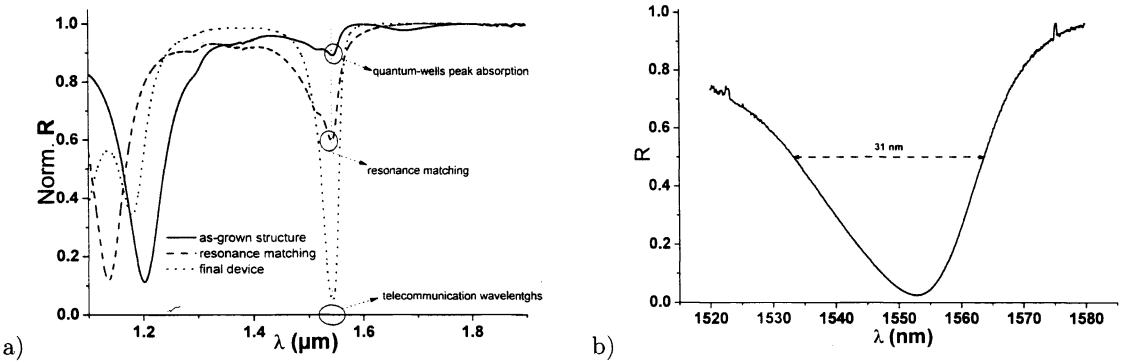

Figure 2. a) Reflection mode optical spectrum measured by FTIR for the as-grown structure (solid line), the resonance matching micro-cavity (dashed line) and the final device (dotted line). b) Final device reflection mode optical spectra measured by an OSA(ASE source). Reflectivities are relative to the gold mirror reflectance.

After the bonding step, the InP substrate is at first mechanically etched, and then completely removed by wet-etching with an 1:1 HCl/H_3PO_3 chemical solution. The InGaAsP etch-stop is also removed by wet-etching with an 3:1:80 $H_3PO_3/H_2O_2/H_2O$ solution. After all these steps we get an asymmetric Fabry-Perot microcavity with a resonance wavelength matching near 1550 nm. To improve the resonance matching, we can slightly etch

the top phase layer. Finally the last step consists in depositing the front mirror. As a too large contrast is not wanted, it is necessary to avoid the perfect impedance matching, i.e a zero low intensity cavity reflectance, got if the relation $R_f = R_t e^{-2\alpha_0 N_{eff}}$ is satisfied, where R_f and R_b are the front and back mirror reflectance, α_0 the absorption coefficient per quantum wells and N_{eff} is the effective number of quantum wells by taking the intracavity intensity enhancement into account. So we chose a 2× TiO_2/SiO_2 [$\lambda/4$, $\lambda/4$] front mirror deposited by EBE and giving a reflectance of 78 %. Figure 2.a shows reflection mode optical spectrum measured by Fourier transform infrared spectroscopy (FTIR) for the as-grown sample, the resonance matching structure and the final device. Figure 2.b shows a more accurate measurement with an optical spectrum analyser (OSA) and a $1/e^2$ beam waist radius of 8 μm. We see that the final device has an optical bandwidth of 31 nm with a working wavelength around 1552nm in resonance with the quantum wells peak absorption. So this device may potentially work on almost all the conventional optical telecommunication wavelength band (C-band, from λ=1530 nm to λ=1565 nm).

3. EXPERIMENTS AND DISCUSSION

The set-up described on figure 3 has been used in order to investigate the nonlinear behavior of this device. A mode-locked source produces ps pulses at 20 MHz, at 1552 nm. The incident pulse, with a 2 nm -3 dB bandwidth, was focused on the sample thanks to a lensed optical fiber with a spot size of 4 μm ($1/e^2$ diameter). The device is used in reflection mode and the output signal is collected back by the lensed optical fiber and then analyzed with a photodetector.

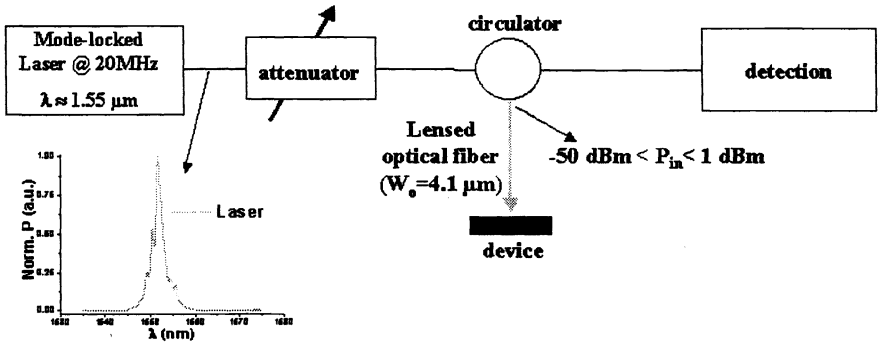

Figure 3. Non-linear optical measurements set-up.

The experimental set-up detects the transfer function, i.e. reflectivity (relative to the gold mirror reflectance) as a function of input energy. Figure 4.a reports a typical transfer function measured with this device. To fit these experimental data, the analytic approximation of equation (1) has been used. It is derived from the semiempirical saturation absorption equation.[26] From this fit, some key parameters can be deduced, such as maximum and minimum reflectivities (R_{max} and R_{min}) corresponding to the passing and blocking state respectively, and the switching energy E_c corresponding to the curve inflexion point. The β parameter, theoretically equals to 1, allows a better data adjustment. From the passing and blocking reflectivity we can calculate the device contrast C defined as $C=10\times\log(R_{max}/R_{min})$, and the device insertion loss IL defined as $IL=10\times\log(1/R_{max})$ (Gold mirror insertion loss are neglected).

$$R = R_{max} + \left(\frac{R_{min} - R_{max}}{1 + \left(\frac{E}{E_c} \right)^{\beta}} \right) \tag{1}$$

To investigate the potential WDM performance of this device, we measured such a transfer function for two different working points on the same device but having a different resonance wavelength (this small inhomogeneity is mainly due to the hand-made wet-etching). We chose two points with a resonance wavelength (λ_{res}) at 1554 nm

and 1547 nm respectively. Measurements have been performed by keeping the laser wavelength at 1552 nm and normalized to a gold mirror reflectance. Results are given on figure 4.a. In both cases we obtain two similar experimental curves with a β value close to 1, showing a good adequation between experimental data and the usual absorption saturation law. Fits give a switching energy of 14 μJ/cm^2 and 13μJ/cm^2, corresponding to an incident average power of about -17.5 dBm at a repetition rate of 20MHz, and a contrast of 9 dB and 8 dB respectively. The main difference consists in insertion loss larger at λ_{res}=1554 nm than at λ_{res}=1547 nm (0.8 dB instead of 0.2 dB). This difference comes from the resonance shape in the passing state. Even if absorption is totally saturated, we still have the interferometric Fabry-Perot effect and consequently some insertion loss. But this effect decreases if we move away from the resonance wavelength as we note with our experimental data when the resonance wavelength moves away from the laser wavelength. But on the other hand, the contrast also decreases and the switching energy increases. Assuming a symmetric reflectivity resonance peak, close to the reality as we may see on the figure 2.b. the device has a bandwidth of 10 nm with a contrast of at least 8 dB, a switching energy around 14 μJ/cm^2 and IL lower than 1 dB (with a minimum of 0.2 dB). We were limited in this investigation by the laser wavelength tunability and the small device inhomogeneity.

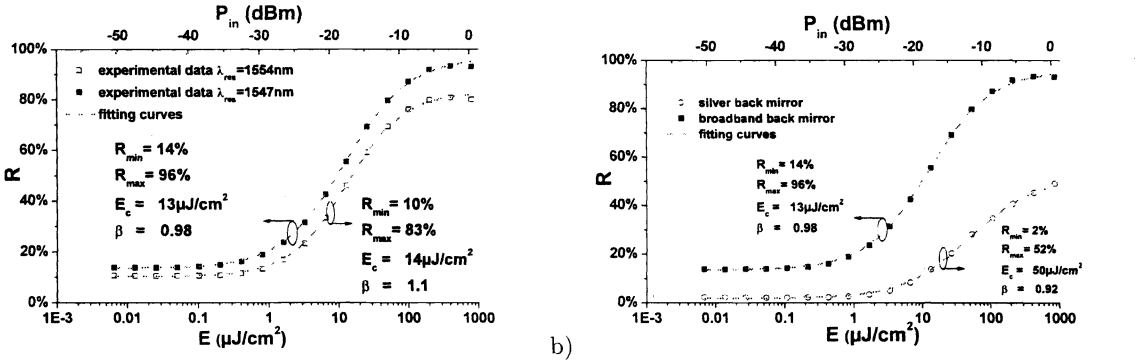

Figure 4. a) Experimental transfer functions measured with the Ag-based broadband back mirror device, at a resonance wavelength of 1547 nm (full square) and 1554 nm (open square) respectively and fitting curves (dashed line). b) Experimental transfer function for a Ag-based broadband back mirror device (full square) and a simple Ag layer back mirror device (open circle). λ_{laser}=1552 nm

To highlight the improvement brought by the silver-based broadband mirror, we made a second device similar to the previous one with the same as-grown structure and the same front mirror but with a simple silver thin layer as the back mirror. Measurements have been done with a laser wavelength at 1552 nm and are plotted on figure 4.b. The difference is quite significant. As expected the use of the high-reflectivity broadband mirror strongly reduces the IL compared to a simple Ag layer. by reducing IL from 3dB to less than 0.8dB. Furthermore as the cavity finesse is increased. the active layer placed at the antinode of the intracavity intensity is subject to a stronger intensity and consequently has a switching energy 4 times lower (13 μJ/cm^2 instead of 50 μJ/cm^2). We note that the Ag layer device has a higher contrast, which is due to a closer impedance matching.

To complete the device characterization, we determined the device response time by pump-probe measurements using a mode-locked laser source producing 1 ps pulses at 23 MHz repetition rate and 1.55 μm wavelength. The response time is defined as the $1/e$ decay time extracted from mono-exponential fitting to the measurements. The measurements, plotted on figure 5, show a response time of 4.8 ps, short enough to achieve signal processing up to 40 Gbit/s.

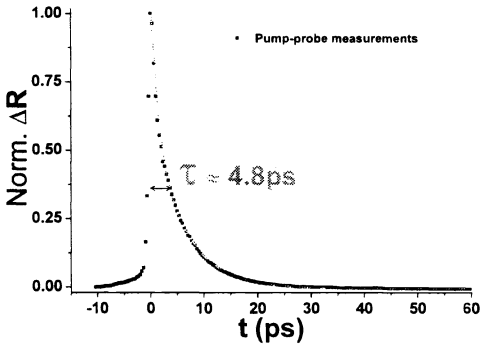

Figure 5. Broadband mirror device normalized probe reflectivity change.

4. CONCLUSION

A vertical-access passive all-optical gate has been fabricated with a high-reflectivity broadband silver-based back mirror. Such a device compared to a silver-thin-layer back mirror device allows to strongly reduce insertion loss and switching energy at the same time, and maintain a large bandwidth and a good contrast. Optical characterization, performed at 1.55 μm, has shown a 10 nm working bandwidth with insertion loss lower than 0.8 dB (with a minimum of 0.2 dB), a contrast of 8 dB and a switching energy of 13 μJ/cm^2. Furthermore, the ion-irradiation provides a device response time lower than 5 ps. These results, the best ever reported to our knowledge for saturable absorber-based switching gate, are very promising for applications in 2 R regenerated WDM transmission lines at high-bit rate.

ACKNOWLEDGMENTS

The authors gratefully acknowledge the help of H. Bernas from CSNSM (Orsay, France) for the ion-irradiation. This work was partially supported by the French Telecom Research Network (RNRT-ASTERIX project).

REFERENCES

1. O. Leclerc, B. Lavigne, E. Balmefrezol, P. Brindel, L. Pierre, D. Rouvillain, and F. Seguineau, "OpticalRegeneration at 40 Gbit/s and Beyond," *J. of Ligthwave Technol.* **21**(11), pp. 2779–2790, 2003.
2. D. Cotter, J. K. Lucek, and D. D. Marcenec, "Ultra-high-bit-rate networking: From the transcontinental backbone to the desktop," *IEEE Comm. Magazine* , pp. 90–95, 1997.
3. O. Leclerc, "Optical vs. Electronic in-line Signal Processing in Optical Communication Systems: An Exciting Challenge for Optical Devices," in *ECIO'03*, 2003.
4. L. Lucek and K. Smith, "All-Optical Signal Regenerator," *Opt. Lett.* **18**(15), pp. 1226–1228, 1993.
5. K. E. Stubkjaer, "Semiconductor Optical Amplifier-Based All-Optical Gates for High-Speed Optical Processing," *IEEE Journal of Selected Topics on Quatum Electronics* **6**(6), pp. 1428–1435, 2000.
6. P. S. Cho, D. Mahgerefteh, and J. Goldhar, "All-Optical 2R Regeneration and Wavelength Conversion at 20 Gb/s Using an Electroabsorption Modulator," *IEEE Photon. Technol. Lett.* **11**(12), pp. 1662–1664, 1999.
7. D. Atkinson, W. H. Loh, V. V. Afanasjev, A. B. Grudinin, A. J. Seeds, and D. N. Payne, "Increased Amplifier Spacing in a Soliton System with Quantum-Well Saturable Absorbers and Spectral Filtering," *Opt. Lett.* **19**(19), pp. 1514–1516, 1994.
8. K. Nonaka, Y. Noguchi, H. Tsuda, and T. Kurokawa, "Digital Signal Regeneration with Side-Injection-Light-Controlled Bistable Laser Diode as a Wavelength Converter," *IEEE Photon. Technol. Lett.* **7**(1), pp. 29–31, 1995.
9. A. Hirano, H. T. Tsuda, K. Hagimoto, R. Takahashi, Y. Kawamura, and H. Iwamura, "10ps Pulse All-Optical Discrimination Using a High-Speed Saturable Absorber Optical Gate," *Electron. Lett.* **31**(9), p. 736, 1995.

10. J. Mangeney, G. Aubin, J. L. Oudar, J. C. Harmand, G. Patriarche, H. Choumane, N. Stelmakh, and J. M. Lourtioz, "All-Optical Discrimination at 1.55 μm Using Ultrafast Saturable Absorber Vertical Cavity Device," *Electron. Lett.* **36**(17), p. 1486, 2000.
11. C. Porzi, A. Isomki, M. Guina, and O. G. Okhotnikov, "Impedance-Detuned High-Contrast Vertical Cavity Semidonductor Switch," in *OFC'2005*, Anaheim, USA, 2005.
12. O. G. Okhotnikov, T. Jouhti, J. Konttinen, S. Karirinne, and M. Pessa, "1.5 μm Monolithic GaInNAs Semiconductor Saturable-Absorber Mode Locking of an Erbium Fiber Laser," *Opt. Lett.* **28**(5), pp. 364–366, 2002.
13. S. Y. Set, H. Yaguchi, M. Jablonski, Y. Tanaka, Y. Sakakibara, A. Rozhin, M. Tokumoto, H. Kataura, Y. Achiba, and K. Kikuchi, "A Noise Suppressing Saturable Absorber at 1550 nm Based on Carbon Nanotube Technology," in *OFC'2003*, Atlanta, USA, 2003.
14. J. L. Oudar, R. Kuszelewicz, B. Sfez, J. C. Michel, and R. Planel, "Prospects for Further Threshold Reduction in Bistable Microresonators," *Opt. Quantum Electron.* **24**(S193), 1993.
15. R. Takahashi, Y. Kawamura, T. Kagawa, and H. Iwamura, "Ultrafast 1.55 μm photoresponses in low-temperature-grown InGaAs/InAlAs quantum wells," *Appl. Phys. Lett.* **65**(14), pp. 1790–1792, 1994.
16. E. L. Delpon, J. L. Oudar, N. Bouche, R. Raj, A. Shen, N. Stelmakh, and J. M. Lourtioz, "Ultrafast excitonic saturable absorption in ion-implanted InGaAs/InAlAs multiple quantum wells," *Appl. Phys. Lett.* **72**(7), pp. 759–761, 1998.
17. L. Qian, S. D. Benjamin, P. W. E. Smith, B. J. Robinson, and D. A. Thompson, "Subpicosecond carrier lifetime in beryllium-doped InGaAsP grown by He-plasma-assisted molecular beam epitaxy," *Appl. Phys. Lett.* **71**(11), pp. 1513–1515, 1997.
18. M. Guezo, S. Loualiche, J. Even, A. L. Corre, O. Dehaese, Y. Pellan, and A. Marceaux, "Nonlinear Absorption Temporal Dynamics of Fe-Doped GaInAs/InP Multiple Quantum Wells," *Journal of Applied Physics* **94**(4), p. 2355, 2003.
19. J. Mangeney, J. Lopez, N. Stelmakh, J.-M. Lourtioz, J.-L. Oudar, and H. Bernas, "Subgap optical absorption and recombination center efficiency in bulk GaAs irradiated by light or heavy ions," *Appl. Phys. Lett.* **76**(1), pp. 40–42, 2000.
20. D. Rouvillain, P. Brindel, F. Seguineau, L. Pierre, O. Leclerc, H. Choumane, G. Aubin, and J. L. Oudar, "Optical 2R Regenerator Based on Passive Saturable Absorber for 40 Gbit/s WDM Long-Haul Transmissions," *Electron. Lett.* **38**(19), p. 1113, 2002.
21. J. Mangeney, S. Barr, G. Aubin, J. L. Oudar, and O. Leclerc, "System Application of 1.5 μm Ultrafast Saturable Absorber in 10 Gbit/s Long-Haul Transmission," *Electron. Lett.* **36**(20), pp. 1725–1727, 2000.
22. D. Massoubre, J. L. Oudar, H. Choumane, G. Aubin, J. C. Harmand, A. Shen, J. Decobert, J. Landreau, and B. Thdrez, "Low Switching Energy Saturable Absorber Device for 40Gbit/s Networks," in *Integrated Photonics Research*, San-Francisco, USA, 2004.
23. D. Massoubre, J. L. Oudar, G. Aubin, J. Dion, A. Shen, J. Decobert, N. Lagay, A. O'Hare, Z. Belfqih, M. Gay, L. Bramerie, S. Seve, E. Lecren, and J. C. Simon, "High Speed, High Switching Contrast Quantum Well Saturable Absorber for 160 Gbit/s Operation," in *CLEO 2005*, Baltimore, USA, 2005.
24. J. Mangeney, H. Choumane, G. Patriarche, G. Leroux, G. Aubin, J. C. Harmand, and J. L. Oudar, "Comparison of light- and heavy-ion-irradiated quantum-wells for use as ultrafast saturable absorbers," *Appl. Phys. Lett.* **79**(17), pp. 2722–2724, 2001.
25. C. C. Lee, C. Y. Wang, and G. Matijasevic, "Au-In Bonding Below the Eutectic temperature," *IEEE Trans. Comp., Hybrids, Manuf Technol.* **16**, pp. 311–316, 1993.
26. D. A. B. Miller, D. S. Chemla, D. J. Eilenberger, P. W. Smith, A. C. Gossars, and W. T. Tsang, "Large room-temperature optical nonlinearity in GaAs/$Ga_{1-x}Al_xAs$ multiple quantum well structures," *Appl. Phys. Lett.* **41**(8), pp. 679–681, 1982.